J Mater Sci: Mater Electron (2017) 28:13217–13228
DOI 10.1007/s10854-017-7157-2

Influence of graphene growth temperature by chemical vapour deposition on the hydrogen response of palladium–graphene junction

D. Dutta[1,2] · J. Das[2] · S. K. Hazra[3] · C. K. Sarkar[1] · S. Basu[1]

Received: 6 March 2017 / Accepted: 15 May 2017 / Published online: 19 May 2017

Abstract The hydrogen sensing by palladium-graphene junction was dependent on the atmospheric pressure chemical vapour deposition growth temperature of the graphene films. The growth temperature window adopted in this study was 900–1000 °C, and the hydrogen sensor performance of the palladium–graphene junction (0.5–2.0% H_2 in air) was studied in the temperature range 30–150 °C. Raman spectroscopy study with the as grown graphene films revealed the multilayer nature and the Pd–graphene planar structure showed a temperature dependent n- to p-type conductivity change in presence of hydrogen. Such a conductivity transition in presence of a reducing gas like hydrogen was experimentally studied in detail, and the hydrogen sensor results were correlated with the multilayer character of the graphene thin film, which induces hydrogen intercalation between the graphene layers.

1 Introduction

Development of chemical gas sensors using graphene thin films is very promising due to its robust nanostructure, very high carrier mobility, high temperature stability and high surface to volume ratio [1]. These unique excellent features of graphene enable precise detection of gases with very low concentrations. Chemical vapour deposition (CVD) is a convenient method to produce graphene in large scale with good layer characteristics for chemical gas sensor applications. The gas response mechanism of graphene based sensor devices is somewhat different from the metal-oxide based gas sensors. Besides the oxidising and reducing features of the target gas molecules during sensing the graphene films have certain other factors that make it attractive for chemical and bio-sensors. Of all the methods that have been previously employed to induce the n-type and p-type behaviour of graphene film, doping is a convenient technique [2]. However, the graphene film can also behave as an n-type or p-type material depending upon the substrate used for its synthesis. The n-type behaviour of graphene deposited on SiO_2/Si substrate as reported by Romero et al., may be due to easy electron transfer from SiO_2 to graphene owing to the lower work function of SiO_2 compared to that of graphene [3]. Sometimes the intercalation of graphene layer by suitable species can also be responsible for the change in conductivity type [2, 4]. Meng et al. in 2013 reported ZnMg and $NbCl_5$ intercalation in the graphene sheet using two-zone vapour transport process resulting in the stable n-type and p-type doping respectively [2]. In 2011 Xue et al. reported the preparation of n-type graphene by mixing CdSe quantum dots with pristine graphene, and p-type graphene by adding tetracyanoethylene (TCNE) molecule on graphene surface [5]. In 2013 Lao et al. reported $FeCl_3$ intercalated graphene. Here the $FeCl_3$ behaves as the electron acceptor (hole doping) [4]. Walter et al. in 2011 reported the synthesis of p-type graphene over the SiC substrate via the fluorine intercalation [6]. Piazza et al. reported the preparation of stable p-type graphene by the exposure of graphene to molecular oxygen at >140 °C [7]. In 2013 Song et al. produced the

✉ S. Basu
sukumarbasu@gmail.com

1 IC Design and Fabrication Centre, Department of ETCE, Jadavpur University, Kolkata 700032, India

2 Department of Physics, Jadavpur University, Kolkata 700032, India

3 Department of Physics and Materials Science, Jaypee University of Information Technology (JUIT), Waknaghat, Himachal Pradesh 173234, India

stable homogeneous p-type graphene film by depositing ZnO thin film over graphene surface using MeV electron beam irradiation method [8]. Huh et al. in 2011 showed n-type doping by decoration of the graphene film using gold nano-particles [9]. Rani et al. showed computationally the existence of p-type and n-type graphene by doping with Boron (B) and Nitrogen (N) atom respectively [10]. The 2D structure of graphene remains unaltered as the size of B, C and N are almost similar. As it is well known, the electron deficient character in B and electron rich character in N create different doping environments [10]. The reversible variation of n- to p-type conductivity is another interesting feature of the graphene film. In 2015 Tu et al. reported the detectable conversion of n- to p-type in reduced graphene oxide by thermal annealing [11]. The presence of electron acceptor groups and electron donor groups results in the p-type and the n-type behaviour of reduced graphene oxide. Kim et al. in 2012 reported the n-type behaviour of graphene upon exposure to hydrogen gas and this behaviour is more prominent with the increase in the number of layers in graphene film [12]. In 2016 Dutta et al. also reported the change in the type of conductivity of multilayer graphene film in presence of hydrogen gas [13]. A plausible mechanism regarding this behavior was explained by H-atom intercalation [13]. Kumar et al. reported that the annealing for few hours using electric current results in n-type conductivity of both monolayer and few layer graphene [14]. The n-type conductivity of graphene is due to the electronic charge transfer from the annealed SiO_2 layer to graphene surface. They also reported that the conductivity changed to p-type with time. Jaaniso et al. reported on the synthesis of graphene over the SiO_2/Si substrate and the temperature dependent oxygen gas sensor response of the prepared graphene layer [15]. They further reported on the oxygen gas response of graphene with n-type conductivity at room temperature and p-type conductivity at higher temperature [15].

In this communication, we present the deposition of the graphene films on the SiO_2/Si substrate at three different temperatures by using the atmospheric pressure chemical vapour deposition (APCVD) method. The nature of graphene layer was confirmed by Raman spectroscopy. A planar device configuration consisting of graphene film and two lateral Palladium (Pd) metal contacts was used to study hydrogen sensing in the temperature range 30–150 °C with different concentrations of hydrogen (0.5–2%) in air. A possible sensing mechanism has been discussed and correlated to hydrogen intercalation in the multilayer graphene.

2 Experimental

2.1 Graphene deposition

Graphene was deposited on the Cu-coated SiO_2/Si dielectric substrates by APCVD method [13, 16]. Mass Flow Controller (MKS type (M100B))/Mass Flow Meter (MKS Type (M10MB)) were used to control the gas flow rates with ±1% of set point accuracy.

A ~300 nm thick catalytic Cu film was deposited on the SiO_2/Si substrates by electron-beam evaporation prior to graphene deposition. Then the Cu coated SiO_2/Si substrates were loaded into CVD chamber. High purity hydrogen (H_2) to nitrogen (N_2) gas ratio of 25:500 (SCCM) was maintained for 1-h to anneal the Cu metal film at the deposition temperature before introducing methane (CH_4) gas. The annealing of Cu metal makes it more flexible to facilitate the grain growth of graphene. A programmable temperature controller was used to precisely control the growth temperature. Methane (CH_4), was introduced into the reactor along with H_2 and N_2 in the ratio 25:10:300 (SCCM) for graphene growth. CH_4 flow was maintained for 8 min at the growth temperature and then it was stopped. The reactor was subsequently cooled down to room temperature. The samples were then taken out of the reaction chamber and the residual copper layer was etched off the substrates using 1(M) ferric chloride ($FeCl_3$) in 1(M) hydrochloric acid (HCl). Figure 1 clearly describes the sequence of graphene

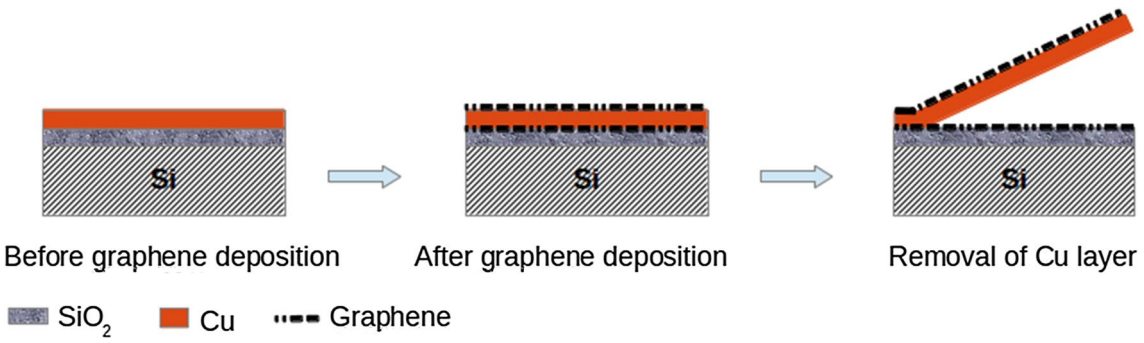

Fig. 1 Schematic of graphene synthesis over SiO_2/Si substrates

growth over SiO_2/Si. The synthesis ultimately ensures the deposition of graphene directly over the SiO_2/Si substrate. The graphene film was deposited on the outer Cu surface and also at the Cu/SiO_2 interface [17]. Three different temperatures (900, 950 and 1000 °C) were selected for the growth of graphene.

2.2 Characterization

Raman spectroscopy was used to study the layer characteristics (multilayer character and defects) of the CVD grown graphene films and the hot probe method was employed to determine the type of electrical conductivity of the grown graphene films.

2.3 Formation of sensor device and electrical contacts

Palladium (Pd) metal contacts of dimension (2 mm × 2 mm) and thickness 0.2 μm were deposited over the graphene surface using e-beam evaporation technique after careful masking for the fabrication of a Pd–graphene–Pd planar structure. Fine copper (Cu) wire and the silver paste were used to complete the electrical contacts. The simple schematic of the sensor structure used in this study is presented below (Fig. 2).

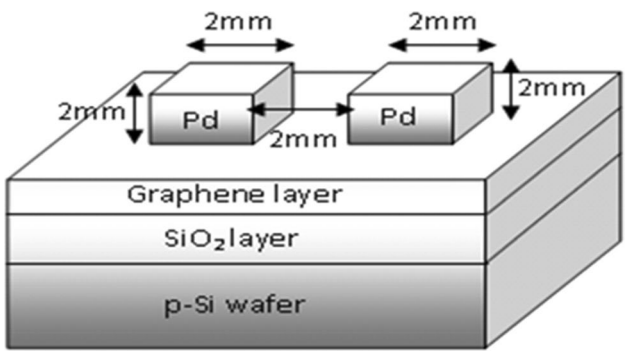

Fig. 2 Schematic diagram of sensor device

2.4 Sensor setup and measurements

The stainless steel gas transmission lines fitted with the mass flow controllers and the mass flow meters (Digiflow, USA) are connected to the Corning glass sensing chamber placed coaxially inside a resistively heated furnace with a 4 cm constant temperature zone [18]. A temperature controller (with ±1 °C accuracy) coupled with a copper constantan thermocouple is used to control the temperature of the chamber. High purity hydrogen (H_2) 99.998%; methane (CH_4) 99.99%; nitrogen (N_2) 99.99% and air [(oxygen ~19.5–23.5%, nitrogen ~76.5–80.5%)] were used for the sensing experiments. A mixing chamber was used to mix the carrier gas and the test gas uniformly prior to introducing into the sensor chamber. The current–voltage characteristics were measured using a Keithley Pico ammeter & voltage source (Model 6487, M/S Keithley Instruments). A schematic of the sensor setup is presented in Fig. 3. The sensor measurements were repeated with different samples obtained from the same batch of the grown graphene films and we obtained ~2% variation in the sensor results showing a small non-uniformity of the graphene layer grown by CVD in our laboratory.

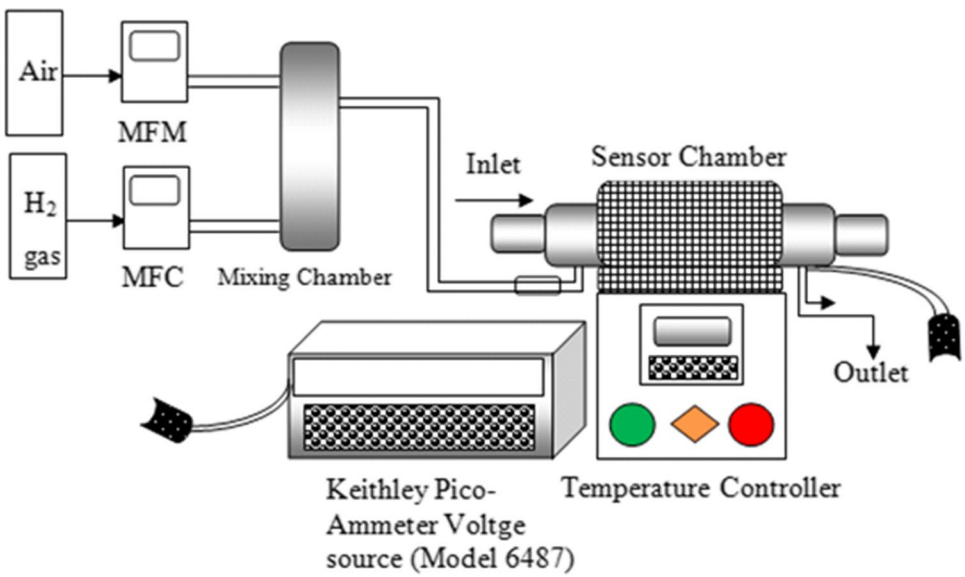

Fig. 3 Schematic diagram of gas sensing assembly

3 Results and discussions

3.1 Raman spectroscopy

Raman spectroscopy has been used to detect the presence of defective carbon networks in the deposited graphene layers [19–21]. Figure 4 displays the Raman spectra of the graphene films grown at three different temperatures (900, 950 and 1000 °C), characterized by the presence of a peak close to 1332 cm^{-1} (the D peak), of a peak close to 1590 cm^{-1} (the G peak) and a further one, also known from literature the 2D one, which varies with the growth temperature from 2650 to 2623 cm^{-1}.

The D-peak at 1332 cm^{-1} is considered in literature to arise from the presence of defects, consisting of vacancies and structural distortions of graphene sheets [19]. The defects may include the vacancies and/or the distortion of graphene sheet that lead to the non-uniformity [22]. The G-peak indicates, instead, the presence of sp^2 hybridized carbon atom. The 2D mode is a second order D mode and its intensity is dependent on the number of layers present in the graphene sample [21, 23]. Since the I_D/I_G peak intensity ratios give information on the defective nature of the grown films, their values have been measured to hold 1.7, 1.4 and 1.6 at 900, 1000 and 1100 °C growth temperatures. The variation of this ratio indicates the variation in defects and quality of the films. I_D/I_G ratio intensity decreased from 1.7 to 1.4 as the growth temperature was increased from 900 to 950 °C but at 1000 °C it increased to 1.6. The probable explanation is the formation of more defects and the increase of graphene layers at higher temperature. Defects increase the surface adsorption of hydrogen and so the increase of gas response. As the graphene growth is accelerated at higher temperature due to the supply of higher thermal energy, more carbon atoms are deposited on the substrate. Both I_D/I_G and I_{2D}/I_G intensity ratios attribute to the higher defect and higher number of graphene layers of the sample grown at 1000 °C. Other researchers also reported the quality of their prepared graphene films by calculating the I_D/I_G and I_{2D}/I_G intensity ratios [22–24]. Huang et al., reported the I_{2D}/I_G intensity ratio of about 1.15 and confirmed the presence of multilayer framework [23]. In our study, the I_{2D}/I_G intensity ratio are 0.61, 0.26, and 0.42 for the graphene samples grown at 900, 950, and 1000 °C respectively indicating the multilayer framework of grown graphene films.

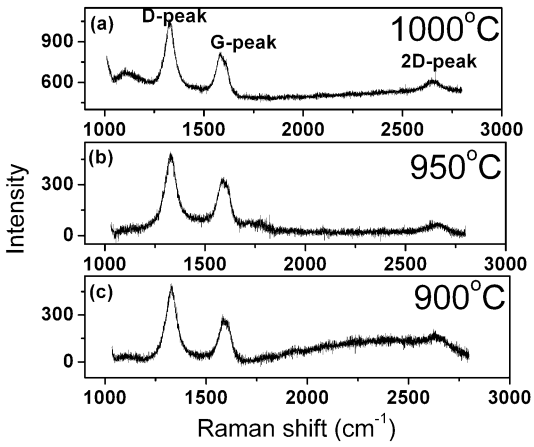

Fig. 4 Raman spectroscopy of graphene grown at **a** 900 °C, **b** 950 °C, and **c** 1000 °C with 8 min CH_4 flow

3.2 Hot probe measurement

Hot Probe is a fast and convenient technique to determine the type of conductivity of a semiconducting material. Hot Probe measurements performed on the graphene samples revealed the n-type conductivity of the samples at room temperature. The change to p-type conductivity in presence of hydrogen mixed with air during the sensor measurements was determined by I–V characteristics, and is discussed in the subsequent section.

3.3 Hydrogen sensor study

The planar device was exposed to different concentrations of hydrogen (0.5, 1.0 and 2.0%) in air. The relative response was calculated as the ratio of change in current in presence of hydrogen mixed with air ($I_g - I_a$) to the initial current in air at a constant voltage and is presented as $[\{(I_g - I_a)/I_a\}_v \times 100]$, where I_g is the current in presence of hydrogen mixed with air and I_a is the current in air. The response time of the sensor was calculated as the time taken by the sensor to reach 90% of its saturation value upon exposure to hydrogen mixed with air and recovery time was calculated as the time corresponding to the decrease of the sensor response by 90% of its saturation value after the hydrogen supply was cut off [18].

The I–V characteristics of the Pd/graphene junction were measured in air and in 2% hydrogen mixed with air for all the three graphene samples (G1, G2 and G3) deposited by CVD for 8 min at three different temperatures.

G1: Pd/graphene junction with graphene film grown at 900 °C.

G2: Pd/graphene junction with graphene film grown at 950 °C.

G3: Pd/graphene junction with graphene film grown at 1000 °C.

The sensor studies were carried out in the temperature range 30–150 °C. Transition of the type of electrical conductivity was observed at a particular temperature during sensing. The transition was determined from the I–V studies, and it was further verified from the transient studies.

It was interesting to observe that the graphene film grown at relatively low temperature (900 °C) manifests the transition close to room temperature during sensing but the transition temperature increases for the graphene films grown at higher temperatures (950 and 1000 °C). Figures 5, 6, and 7 present the I–V curves for G1, G2, and G3 samples respectively. G1 sensor sample shows distinct p-type conductivity from 40 °C onwards. Basically the decrease of the device current in presence of hydrogen gas indicates the p-type behaviour of graphene sample. Although as grown

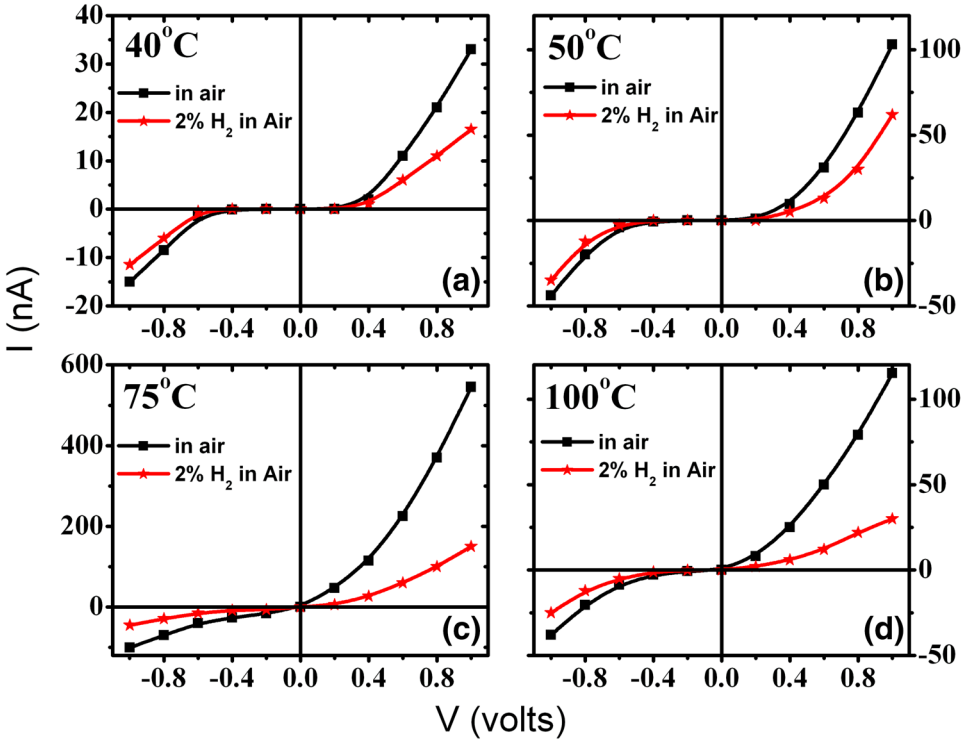

Fig. 5 I–V characteristics of the G1 sample in air and in 2% H_2 mixed with air at different temperatures (p-type response from 40 °C during hydrogen sensing)

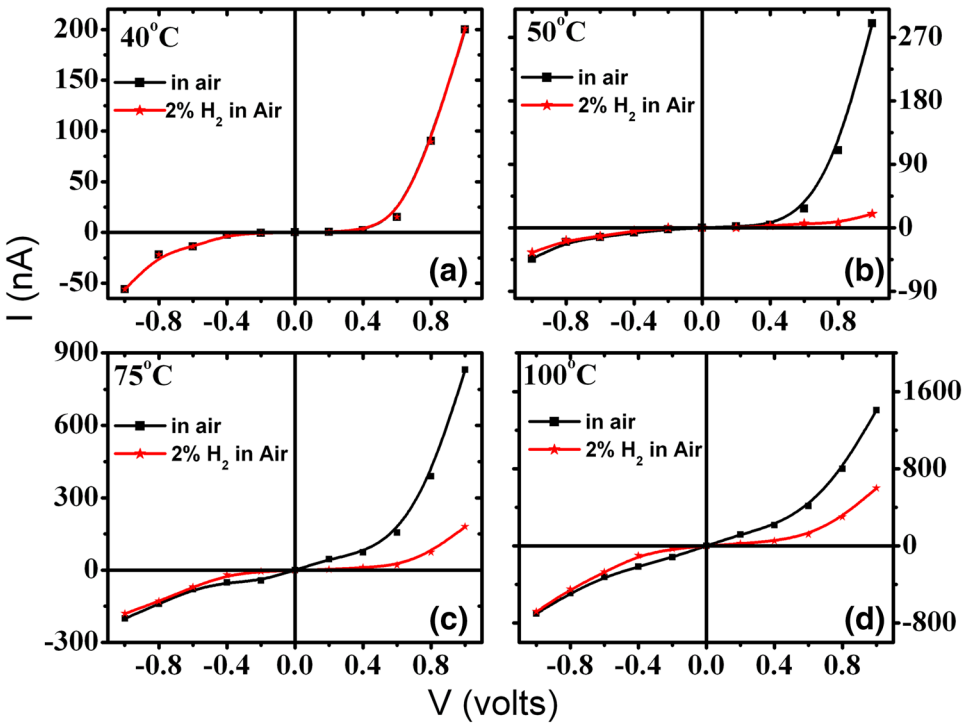

Fig. 6 I–V characteristics of G2 in air and 2% H_2 mixed with air at different temperatures (n-type to p-type inversion at 50 °C during hydrogen sensing)

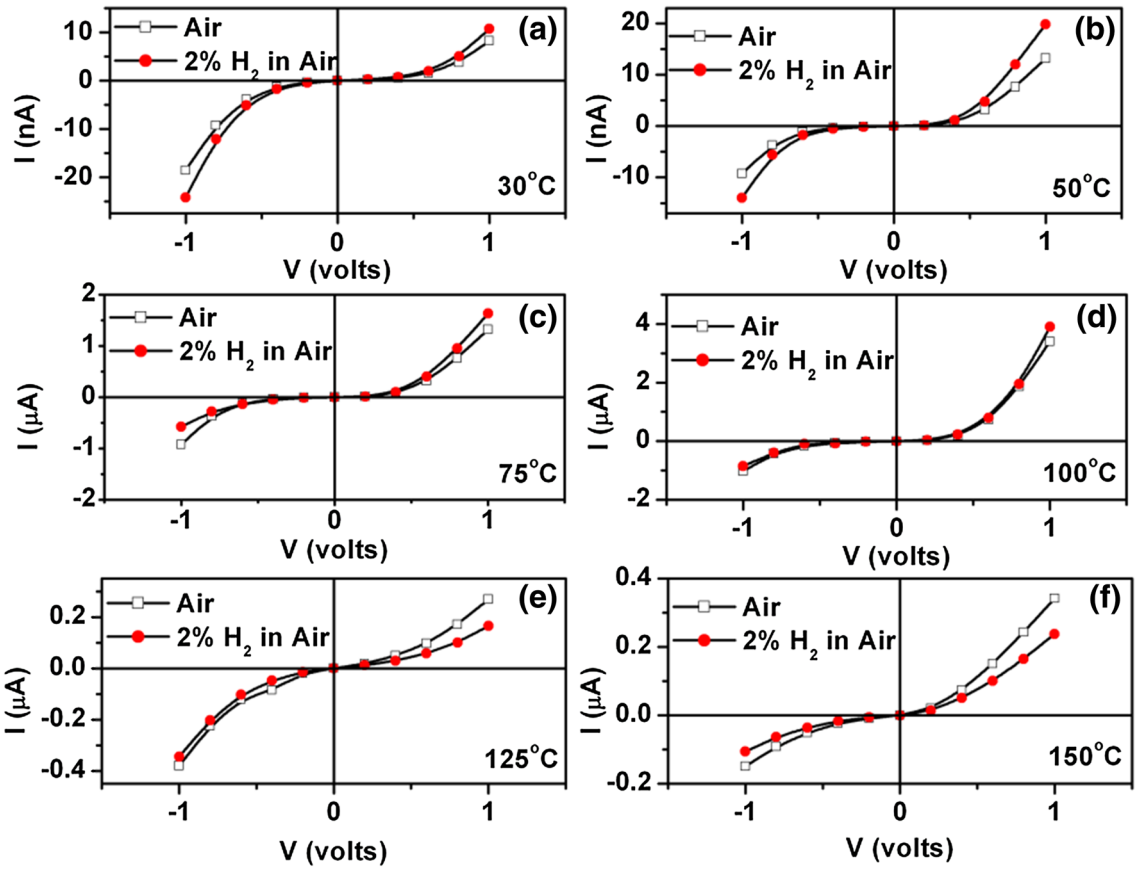

Fig. 7 I–V characteristics of G3 in air and in 2% H_2 in air at different temperatures (n-type to p-type inversion at temperature > 100 °C during hydrogen sensing)

G1 is n-type conducting at 30 °C (obtained from hot probe data), it shows distinct p-type response with the increase in temperature (~40 °C) during sensing. It is worth mentioning here that the G1 samples were not responsive to hydrogen near 30 °C. I–V study of G1 performed in the temperature range 40–100 °C is shown in Fig. 5. The graphene film prepared at 900 °C has less number of layers which is responsible for early p-type response. This is further discussed in the subsequent section to suggest the mechanism of sensing.

For G2 sample no response was found at 30 °C and the response at 40 °C was weakly n-type. But it shows distinct p-type response from 50 °C and above. This is clearly revealed from the I–V studies of G2 (Fig. 6) performed in the temperature range 40–100 °C. The current starts to decrease in presence of hydrogen gas from 50 °C and we obtained the p-type gas response. The shift of the n-/p-transition to higher temperature for G2 can again be attributed to the larger number of layers (more multilayer character) in graphene.

I–V characteristics of G3 samples, shown in Fig. 7, display the initial response to be n-type at 30 °C because the current increases upon exposure to hydrogen in air. When the sensing temperature is raised to 125 °C the current starts decreasing upon exposure to hydrogen in air. This signifies that the n-/p-transition occurs in the temperature range 100–125 °C.

The repeated cycle measurements and the transient response of the graphene sensors were performed in the temperature range 40–100, 50–100 and 30–150 °C for G1 (shown in Fig. 8), G2 (shown in Fig. 9) and G3 (shown in Fig. 10) samples respectively using different H_2 concentrations mixed with air.

The repeated cycle measurements reveal the reproducibility of the response pattern at a particular temperature. The sensor parameters calculated from Figs. 8, 9 and 10 are presented in Fig. 11. It can be noted that all the graphene samples (G1, G2 and G3) show increase in gas response with the increase in hydrogen gas concentrations in air from 0.5 to 2%. This can be due to increase in the surface adsorption because of higher hydrogen partial pressure.

The response time for G3 sample is low (i.e. faster response) on either side of the n- to p-transition temperature range (100–125 °C). This can be correlated to the gas

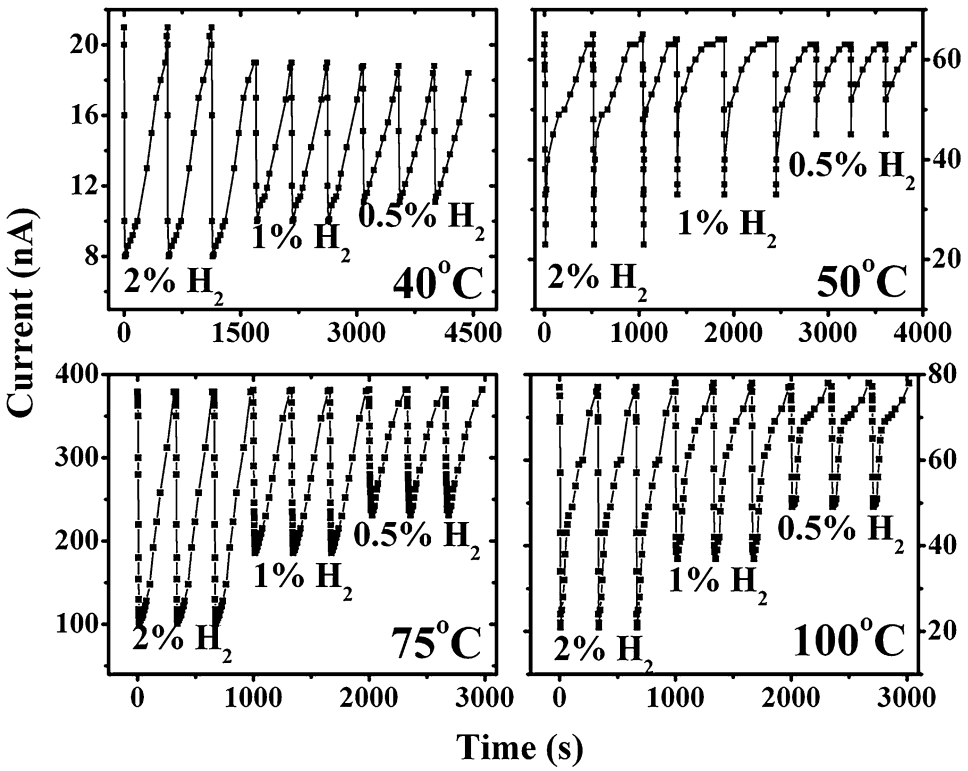

Fig. 8 Repeated cycle and transient responses for different hydrogen concentrations mixed with air with G1 sample

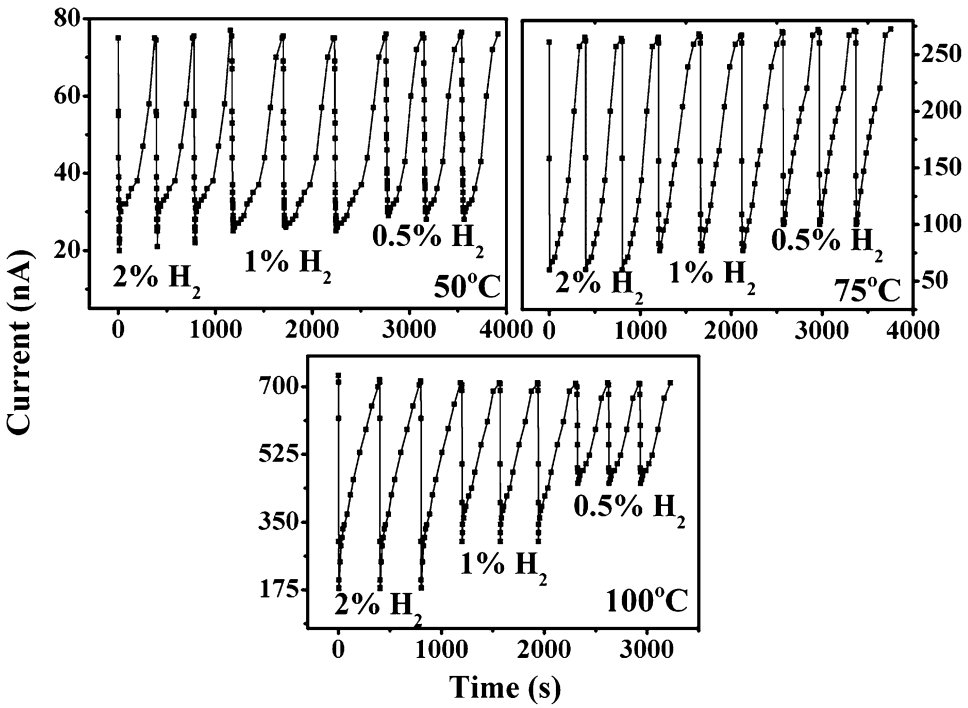

Fig. 9 Repeated cycle and transient responses for different hydrogen concentrations mixed with air with G2 sample

adsorption at a particular operating temperature. In this temperature zone, the % response normally maximizes and the time of response is minimized due to fast adsorption. At the optimum temperature the adsorption is very high, because the active surface of the device can trap maximum number of gas molecules in a very short time period. As a result, the current saturates quickly and the magnitude of current change is large. So, the % response is high and the time of response is short. Beyond the optimum temperature the effect of desorption dominates the

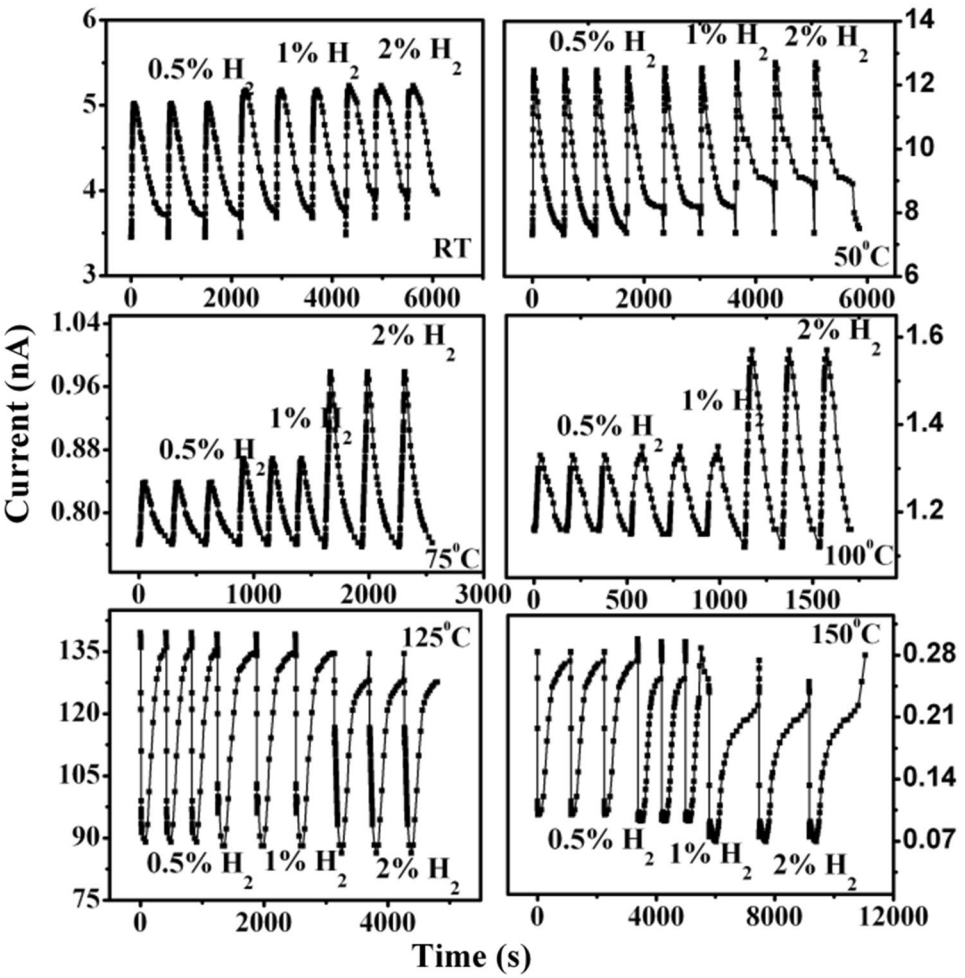

Fig. 10 Repeated cycle and transient responses for different hydrogen concentrations mixed with air with G3 sample

adsorption phenomenon and the current stabilizes after relatively longer time due to the competitive effect of adsorption and desorption occurring almost concurrently. Hence the time of response increases.

Such an optimization of the response parameters is clearly observed in both n- and p-sides of G3 sample. The observed p-side response was faster than the n-side response and it further increased with the increasing temperature. This is due to the fact that the p-type activity is prevalent at relatively higher temperature, which provides sufficient thermal energy for enhanced adsorption and relatively quick current saturation. Hence the thermal energy mainly governs the speed of response. For G1 and G2 samples, the n-side temperature range is negligibly small. Hence the optimization of the response parameters is observed on the p-side. Also for G1 and G2, the p-side optimization occurs within a small temperature range 40–100 °C. Beyond 100 °C the hydrogen response deteriorates. Therefore, the G1 and G2 category samples are good for low temperature sensing and G3 sample is excellent for high temperature applications.

Our earlier study showed excellent stability and good selectivity of Pd/graphene/Pd sensor structure for hydrogen in presence of methane, another reducing gas [13].

The hydrogen sensing results of Pd/graphene/Pd planar structures at different temperatures are presented in Fig. 10. Hot probe measurements at room temperature confirmed n-type electrical conductivity of all the graphene samples, G1, G2 and G3. Our hydrogen sensor results indicate a transition from n-type to p-type conductivity with the increasing sensing temperature and in the presence of hydrogen. However, this transition occurs at much lower temperatures for the graphene samples (G1 and G2) grown by CVD at 900 and 950 °C and at higher temperature for the sample (G3) grown at 1000 °C. This may be directly related to the multilayer character of the graphene samples and the hydrogen intercalation, which is proportional to the increase of multilayer nature. Since the n-/p-transition temperatures for G1 and G2 are almost near the room temperature we did not observe any hydrogen response near room temperature. Therefore, the sensor parameters have been plotted from 50 °C. For G3 sample grown at 1000 °C

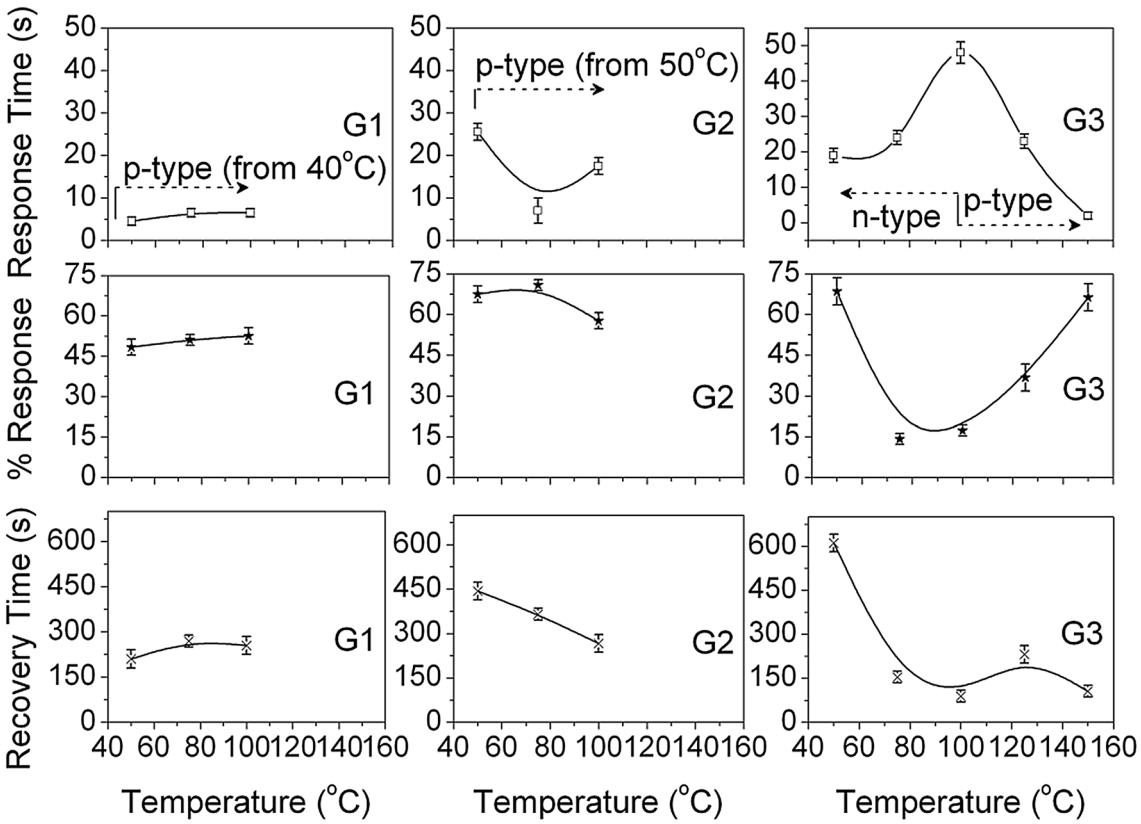

Fig. 11 Response time, % response, and recovery time for hydrogen sensing (1% H_2 in air) with the CVD grown graphene samples at different temperatures

the n-/p-transition occurs at the temperature > 100 °C and therefore we could show the sensing parameters for both n-type and p-type conductivity. From the plots it is apparent that the % response, response time and recovery time of the G3 sample with p-type conductivity are most favourable at 150 °C. It is also worth mentioning that the graphene samples grown at 900 and 950 °C could not sense hydrogen above 100 °C and the devices were deteriorated. So, it appears from our study that CVD grown graphene can sense hydrogen in air at low temperature and also at high temperature depending upon the temperature of deposition of the graphene thin film. However, further study is necessary to find out the exact mechanism of such behaviour.

3.4 Sensing mechanism

Normally, the reason for increase in current is due to reduction in work function of palladium (Pd) metal after dissolution of H-atom into the Pd-bulk. This leads to the lowering of the Pd/graphene interface barrier and an easy electron transfer to graphene thereby increasing the current in presence of hydrogen gas [18, 25]. In this study G1 and G2 graphene samples with n-type conductivity did not show any hydrogen gas response at 30 °C. However, they showed p-type conductivity and hydrogen gas response characteristics at 40 and 50 °C. But for G3 graphene samples we observed n-type conductivity and hydrogen response in the temperature range 30–100 °C.

A single layer graphene is reported to have a work function of 4.55 eV [26], and this work function value decreases with the increase of the multilayer characters of graphene. However, with Pd contact, the work function of graphene is ~4.62 eV [27]. This work function (~4.62 eV) of palladium contacted graphene is expected to vary (i.e. decrease) with the increase in the number of layers of the graphene matrix.

Our samples show increasing trend in the multilayer character with the increase in CVD growth temperature [28]. For instance, G1 samples (grown at 900 °C) have less number of layers than G2 (grown at 950 °C), and G3 (grown at 1000 °C). Hence, it can be said that G1 should have the highest work function (say ~4.62 eV) among the three. Considering the work function of Pd (~5.12 eV), G1, G2, and G3 graphene films should form Schottky contact with palladium. We observed that the CVD grown graphene samples are n-doped due to the effect of SiO_2/Si substrate with the work function of SiO_2 less than graphene [3]. Therefore, upon hydrogen adsorption, the work function of Pd decreases thereby reducing the work function difference

between graphene and palladium, and thus lowering the interface barrier for all the three samples [Fig. 12]. As a result, the current increases, and a Pd/n-graphene device is supposed to show n-type hydrogen response.

The conductivity transition of graphene from n-type to p-type during hydrogen sensing has been reported in our earlier study [13] and various mechanisms have been discussed. According to our present experimental results, the intercalation of the graphene layer, starting at a particular temperature, can possibly be the dominating phenomenon responsible for the reversal of n-type character. Basically, intercalation by hydrogen refers to the temporary isolation of the graphene layer from the substrate due to presence of hydrogen atoms at the interface (Fig. 13). This leads to the trapping of generated electrons by the interface oxygen radicals and hence the p-type behavior is observed [13]. As a matter of fact, thermal energy and interfacial oxygen states play the most important role in this intercalation phenomenon. And both these parameters vary with the multilayer character of graphene. For instance, amount of hydrogen required to purge the interface of perfect monolayer graphene is relatively lower than that required for a defective multilayered structure.

Since gas adsorption is a temperature controlled phenomenon the intercalation for monolayer graphene may happen at lower temperature than that for defective multilayer graphene, where higher adsorption requires relatively higher operational temperatures and a large number of hydrogen atoms can be made available at the interface. We have confirmed from Raman spectroscopy, AFM and TEM that the multilayer character of graphene increases with increasing CVD growth temperature in the order G1 < G2 < G3 [28].

The required temperature to have intercalation and p-type behavior in G1 should be relatively lower than G2 and G3 in the order G1 < G2 < G3. Therefore, we obtained p-type hydrogen response from 40, 50, and >100 °C for G1, G2, and G3 samples, respectively. This implies that the interface energy band alignment due to this inversion of the type of electrical conductivity starts changing from these temperatures. Upon hydrogen adsorption, the work function of Pd decreases and the work function difference between graphene and palladium increases, leading to the increase of the interface barrier for G1,G2 and G3 samples (Fig. 11). As a result, the current decreases and the p-type hydrogen response is observed at the Pd/graphene interface.

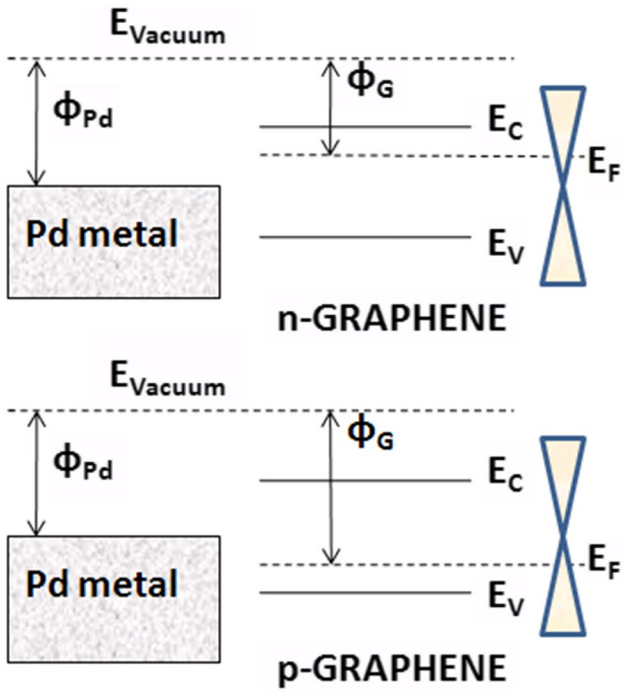

Fig. 12 Interface band shift of Pd/graphene junctions due to hydrogen intercalation (ϕ_{Pd} and ϕ_G are workfunctions of palladium and graphene respectively; E_C, E_F, and E_V are energy levels corresponding to conduction band, Fermi level, and valence band respectively)

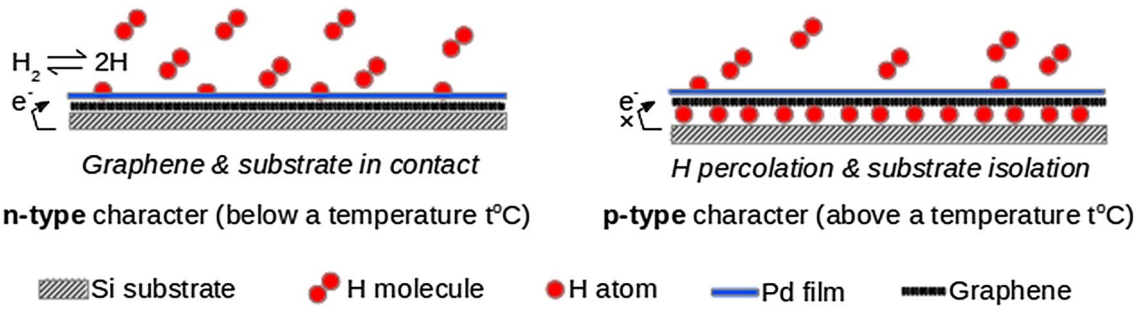

Fig. 13 Intercalation phenomenon in the graphene layers of the sensor devices in hydrogen ambient (t °C is the minimum temperature at which intercalation starts)

4 Conclusion

Hydrogen sensing by multilayer graphene films grown by CVD is a complex phenomenon which could be explained taking into account the hydrogen intercalation in the multilayer graphene structure along with the thermodynamics and kinetics of gas adsorption/desorption processes, and the kinetics of charge transfer through the metal-graphene interface during p-/n-transition. Our experimental observations reveal that the hydrogen sensing temperature of CVD grown graphene thin films is related with the multilayer character, which is a function of CVD growth temperature. In this study an attempt has been made to explain the hydrogen sensing behaviour of the graphene samples grown by chemical vapour deposition at three different temperatures. Based on our observations and interpretations of the experimental results we may come to the following conclusions;

1. CVD grown graphene film on SiO_2/Si dielectric substrates can be a promising material for hydrogen sensing at different temperatures.
2. Transition of the electrical conductivity of graphene from n-type to p-type in presence of hydrogen controls the hydrogen sensing characteristics.
3. Intercalation of hydrogen in the layer structure of graphene during sensing plays a vital role in the sensor response.

Acknowledgements D. Dutta thankfully acknowledges CSIR, Govt. of India for providing a research fellowship to carry out the work. S. K. Hazra is thankful to IC Design & Fabrication Centre, Dept. of ETCE, Jadavpur University, India for providing the collaborative research opportunity. The authors are thankful to Prof. E. Bontempi, (INSTM and Dipartimento di Ingegneria Meccanica ed Industriale), Brescia University, Italy for providing Raman results of our graphene samples.

References

1. S. Basu, P. Bhattacharyya, Recent developments on graphene and graphene oxide based solid state gas sensors. Sens. Actuators B **173**, 1–21 (2012)
2. X. Meng, S. Tongay, J. Kang, Z. Chen, F. Wu, S.S. Li, J.B. Xia, J. Li, J. Wu, Stable p- and n-type doping of few-layer graphene/graphite. Carbon **57**, 507 (2013)
3. H.E. Romero, N. Shen, P. Joshi, H.R. Gutierrez, S.A. Tadigadapa, J.O. Sofo, P.C. Eklund, n-Type behavior of graphene supported on Si/SiO_2 substrates. ACS Nano **2**, 2037–2044 (2008)
4. Y.F. Lao, A.G.U. Perera, K. Shepperd, F. Wang, E.H. Conrad, M.D. Williams, Temperature-dependent far-infrared response of epitaxial multilayer graphene. Appl. Phys. Lett. **102**, 231906 (2013)
5. H.Y. Xue, G.X. Mei, L.Y. Zuo, D. Bin, L.L. Wei, S.M. Tao, Electrical and Raman properties of p-type and n-type modified graphene by inorganic quantum dot and organic molecule modification. Sci. China Phys. Mech. Astron. **54**(**3**), 416–419 (2011)
6. A.L. Walter, K.J. Jeon, A. Bostwick, F. Speck, M. Ostler, T. Seyller, L. Moreschini, Y.S. Kim, Y.J. Chang, K. Horn, E. Rotenberg, Highly p-doped epitaxial graphene obtained by fluorine intercalation. Appl. Phys. Lett. **98**, 184102 (2011)
7. A. Piazza, F. Giannazzo, G. Buscarino, G. Fisichella, A.L. Magna, F. Roccaforte, M. Cannas, F.M. Gelardi, S. Agnello, Graphene p-type doping and stability by thermal treatments in molecular oxygen controlled atmosphere, J. Phys. Chem. C **119**(39), 22718–22723 (2015)
8. W. Song, Y. Kim, S.H. Kim, S.Y. Kim, M. Cha, I. Song, D.S. Jung, C. Jeon, T. Lim, S. Lee, S. Ju, W.C. Choi, M.W. Jung, K. An, C. Park, Homogeneous and stable p-type doping of graphene by MeV electron beam-stimulated hybridization with ZnO thin films. Appl. Phys. Lett. **102**, 053103 (2013)
9. S. Huh, J. Park, K.S. Kim, B.H. Hong, S.B. Kim, Selective n-type doping of graphene by photo-patterned gold nanoparticles, ACS Nano **5**(5), 3639–3644 (2011)
10. P. Rani, V.K. Jindal, Designing band gap of graphene by B and N dopant atoms. RSC Adv. **3**, 802–812 (2013)
11. N.D.K. Tu, J. Choi, C.R. Park, H. Kim, Remarkable conversion between n- and p-type reduced graphene oxide on varying the thermal annealing temperature. Chem. Mater. **27**, 7362–7369 (2015)
12. B.H. Kim, S.J. Hong, S.J. Baek, H.Y. Jeong, N. Park, M. Lee, S.W. Lee, M. Park, S.W. Chu, H.S. Shin, J. Lim, J.C. Lee, Y. Jun, Y.W. Park, n-type graphene induced by dissociative H_2 adsorption at room temperature, Sci. Rep. (2012). doi:10.1038/srep00690
13. D. Dutta, S.K. Hazra, J. Das, C.K. Sarkar, S. Basu, Temperature- and hydrogen-gas-dependent reversible inversion of n-/p-type conductivity in CVD-grown multilayer graphene (MLG) film, J. Electron. Mater. **45**(6), 2861–2869, (2016)
14. P. Kumar, A. Kumar, Carrier type modulation in current annealed graphene layers. Appl. Phys. Lett. **104**, 083517 (2014)
15. R. Jaaniso, T. Kahro, J. Kozlova, J. Aarik, L. Aarik, H. Alles, A. Floren, A. Gersta, A. Kasikov, A. Niiliska, V. Sammelselg, Temperature induced inversion of oxygen response in CVD graphene on SiO_2. Sens. Actuators B **190**, 1006–1013 (2014)
16. D. Dutta, A. Hazra, J. Das, S. K. Hazra, V.N. Lakshmi, S.K. Sinha, A. Gianonchelli, C.K. Sarkar, S. Basu, Growth of multilayer graphene by chemical vapor deposition (CVD) and characterizations, J. Nano Sci. Mol. Nanotechnol. (2013). doi:10.4172/2324-8777.S1-004
17. C.Y. Su, A.Y. Lu, C.Y. Wu, Y.T. Li, K.K. Liu, Z. Zhang, S.Y. Lin, Z.Y. Juang, Y.L. Zhong, F.R. Chen, L.J. Li, Direct formation of wafer scale graphene thin layers on insulating substrates by chemical vapor deposition. Nano Lett. **11**, 3612–3616 (2011)
18. D. Dutta, S.K. Hazra, J. Das, C.K. Sarkar, S. Basu, Studies on p-TiO_2/n-graphene heterojunction for hydrogen detection. Sens. Actuators B **212**, 84 (2015)
19. A. Das, B. Chakraborty, A.K. Sood, Raman spectroscopy of graphene on different substrates and influence of defects. Bull. Mater. Sci. **31**, 579–584 (2008)
20. W. Liu, H. Li, C. Xu, Y. Khatami, K. Banerjee, Synthesis of high-quality mono layer and bi layer graphene on copper using chemical vapor deposition. Carbon **49**, 4122–4130 (2011)
21. M.H. Rummeli, A. Bachmatiuk, A. Scott, F. Rrnert, J.H. Warner, V. Hoffman, J.H. Lin, G. Cuniberti, B. Buchner, Direct low-temperature nano graphene CVD synthesis over a dielectric insulator. ACS Nano **4**, 4206–4210 (2010)

22. J.J. Wang, M.Y. Zhu, R.A. Outlaw, X. Zhao, D.M. Manos, B.C. Holloway, Free-standing sub nanometer graphite sheets. Appl. Phys. Lett. **85**, 1265–1267 (2004)
23. L. Huang, Q.H. Chang, G.L. Guo, Y. Liu, Y.Q. Xie, T. Wang, B. Ling, H.F. Yang, Synthesis of high-quality graphene films on nickel foils by rapid thermal chemical vapor deposition. Carbon **50**, 551–556 (2012)
24. A. Ismach, C. Druzgalski, S. Penwell, A. Schwartzberg, M. Zheng, A. Javey, J. Bokor, Y. Zhang, Direct chemical vapor deposition of graphene on dielectric surfaces. Nano Lett. **10**, 1542–1548 (2010)
25. U. Langea, T. Hirsch, V. Mirsky, O. Wolfbeis, Hydrogen sensor based on a graphene palladium nanocomposite. Electrochim. Acta **56**, 3707–3712 (2011)
26. V. Panchal, R. Pearce, R. Yakimova, A. Tzalenchuk, O. Kazakova, Standardization of surface potential measurements of graphene domains, Sci. Rep. **3**, 2597 (2013)
27. S.M. Song, J.K. Park, O.J. Sul, B.J. Cho, Determination of work function of graphene under a metal electrode and its role in contact resistance, Nano Lett. **12**(8) 3887–3892, (2012). doi:10.1021/nl300266p.
28. D. Dutta, E. Bontempi, Y. You, S. Sinha, J. Das, S.K. Hazra, C.K. Sarkar, S. Basu, Surface topography and hydrogen sensor response of APCVD grown multilayer graphene thin films. J. Mater. Sci. (2016). doi:10.1007/s10854-016-5506-1